

## **Exenatide induces frataxin expression and improves mitochondrial function in Friedreich ataxia**

Mariana Igoillo-Esteve<sup>1\*</sup>, Ana F Oliveira<sup>1</sup>, Cristina Cosentino<sup>1</sup>, Federica Fantuzzi<sup>1</sup>, Céline Demarez<sup>1</sup>, Sanna Toivonen<sup>1</sup>, Amélie Hu<sup>2</sup>, Satyan Chintawar<sup>2,3</sup>, Miguel Lopes<sup>1</sup>, Nathalie Pachera<sup>1</sup>, Ying Cai<sup>1</sup>, Baroj Abdulkarim<sup>1</sup>, Myriam Rai<sup>2</sup>, Lorella Marselli<sup>4</sup>, Piero Marchetti<sup>4</sup>, Mohammad Tariq<sup>5</sup>, Jean-Christophe Jonas<sup>5</sup>, Marina Boscolo<sup>6</sup>, Massimo Pandolfo<sup>2</sup>, Décio L Eizirik<sup>1</sup>, Miriam Cnop<sup>1,6\*</sup>

<sup>1</sup>ULB Center for Diabetes Research, Faculty of Medicine, Université Libre de Bruxelles, Brussels, Belgium;

<sup>2</sup>Laboratory of Experimental Neurology, Université Libre de Bruxelles, Brussels, Belgium;

<sup>3</sup>Current affiliation: Translational Molecular Neuroscience Group, Weatherall Institute of Molecular Medicine, Nuffield Department of Clinical Neurosciences, University of Oxford, Oxford, UK;

<sup>4</sup>Department of Clinical and Experimental Medicine, University of Pisa, Pisa, Italy;

<sup>5</sup>Université catholique de Louvain, Institute of experimental and clinical research, Pole of endocrinology, diabetes and nutrition, Brussels, Belgium;

<sup>6</sup>Division of Endocrinology, Erasmus Hospital, Université Libre de Bruxelles, Brussels, Belgium

\*Correspondence to: Mariana Igoillo-Esteve or Miriam Cnop

ULB Center for Diabetes Research, Université Libre de Bruxelles CP-618, Route de Lennik 808, 1070 Brussels, Belgium.

Tel: 32.2.555.63.05; Fax: 32.2.555.62.39

Email: migoillo@ulb.ac.be or mcnop@ulb.ac.be

# Supplementary Figure 1

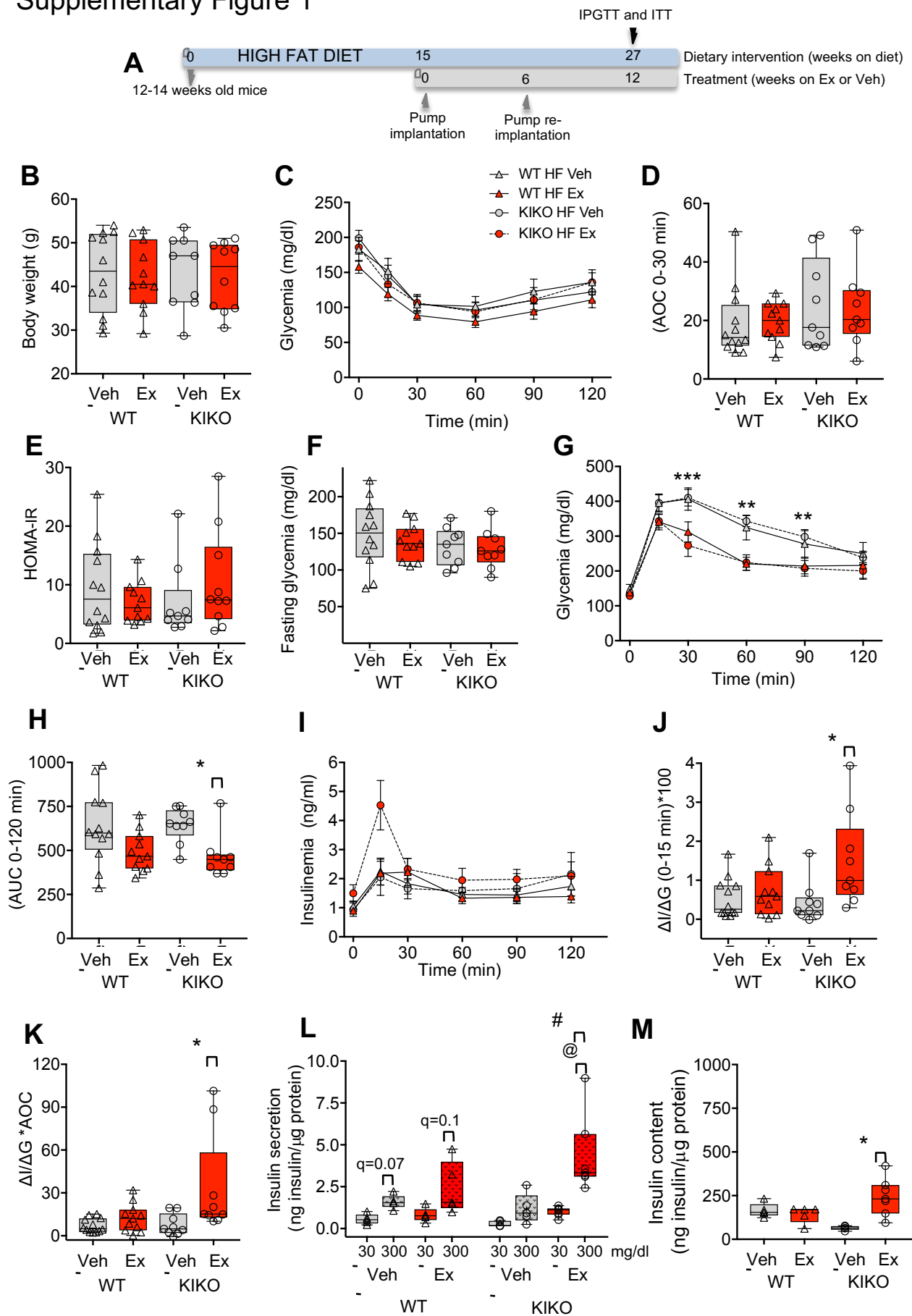


**Figure S1. Exenatide improves glucose tolerance and  $\beta$ -cell function of metabolically stressed KIKO mice.** (A) 12-14-week-old WT and KIKO mice were fed a high fat (HF) diet for 15 weeks and were then randomized to exenatide (Ex) or vehicle (Veh) while keeping the dietary intervention (n=9-12 per group). The following assessments were made at the end of the study: (B) Body weight. (C) Glycemia during the ITT. Insulin sensitivity was quantified as AOC during the ITT (D) and HOMA-IR (E). (F) Fasting glycemia (after 16-hour fast). (G) Glycemia, (H) AUC for glucose and (I) insulin levels during the IPGTT. (J) Insulinogenic index, calculated as  $\Delta I/\Delta G$  in the first 15 min of the IPGTT. (K)  $\beta$ -cell function calculated as insulinogenic index corrected for insulin sensitivity. *Ex vivo* mouse islet glucose-stimulated insulin secretion (L) and insulin content (M) corrected for total protein (n=5-7 per group). Data points correspond to individual mice. The median is shown by a horizontal line in the box plots; 25<sup>th</sup> and 75<sup>th</sup> percentiles are at the bottom and top of the boxes; whiskers represent minimum and maximum values. # $q < 0.05$  KIKO vs WT, \* $q < 0.05$ , \*\* $q < 0.01$ , \*\*\* $q < 0.001$  Veh vs Ex, @ $q < 0.05$ , @@ $q < 0.01$  300 mg/dl vs 30 mg/dl glucose, by Kruskal-Wallis test followed by Benjamini, Krieger and Yekutieli correction for multiple comparisons, or by multiple unpaired t-tests (one per time point, panels C, G and I) followed by Holm-Sidak correction for multiple comparisons.

## Supplementary Figure 2

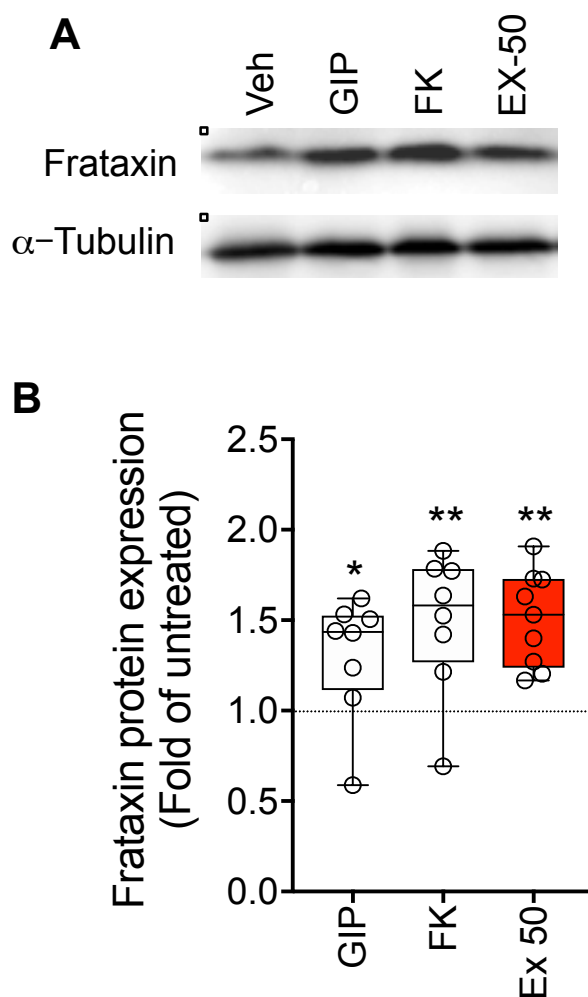


**Figure S2. Exenatide enhances frataxin protein expression in  $\beta$ -cells.** Clonal rat INS-1E  $\beta$ -cells were treated or not (Veh) for 24 hours with the GIP analog [D-Ala<sup>2</sup>]GIP<sub>1-42</sub> (100 nM, GIP), forskolin (20 mM, FK) or exenatide (50 nM, Ex 50). (A) Representative Western blot image and (B) densitometric quantification of frataxin protein expression normalized to  $\alpha$ -tubulin and expressed as fold of the untreated samples (dashed line) (n=8-9 per condition). The horizontal line in the box plots corresponds to the median, 25<sup>th</sup> and 75<sup>th</sup> percentiles are at the bottom and top of the boxes; whiskers indicate minimum and

maximum values. Data points represent independent experiments. \* $q < 0.05$ , \*\* $q < 0.01$  treated vs untreated by one-way ANOVA followed by Benjamini, Krieger and Yekutieli correction for multiple comparisons.

# Supplementary Figure 3

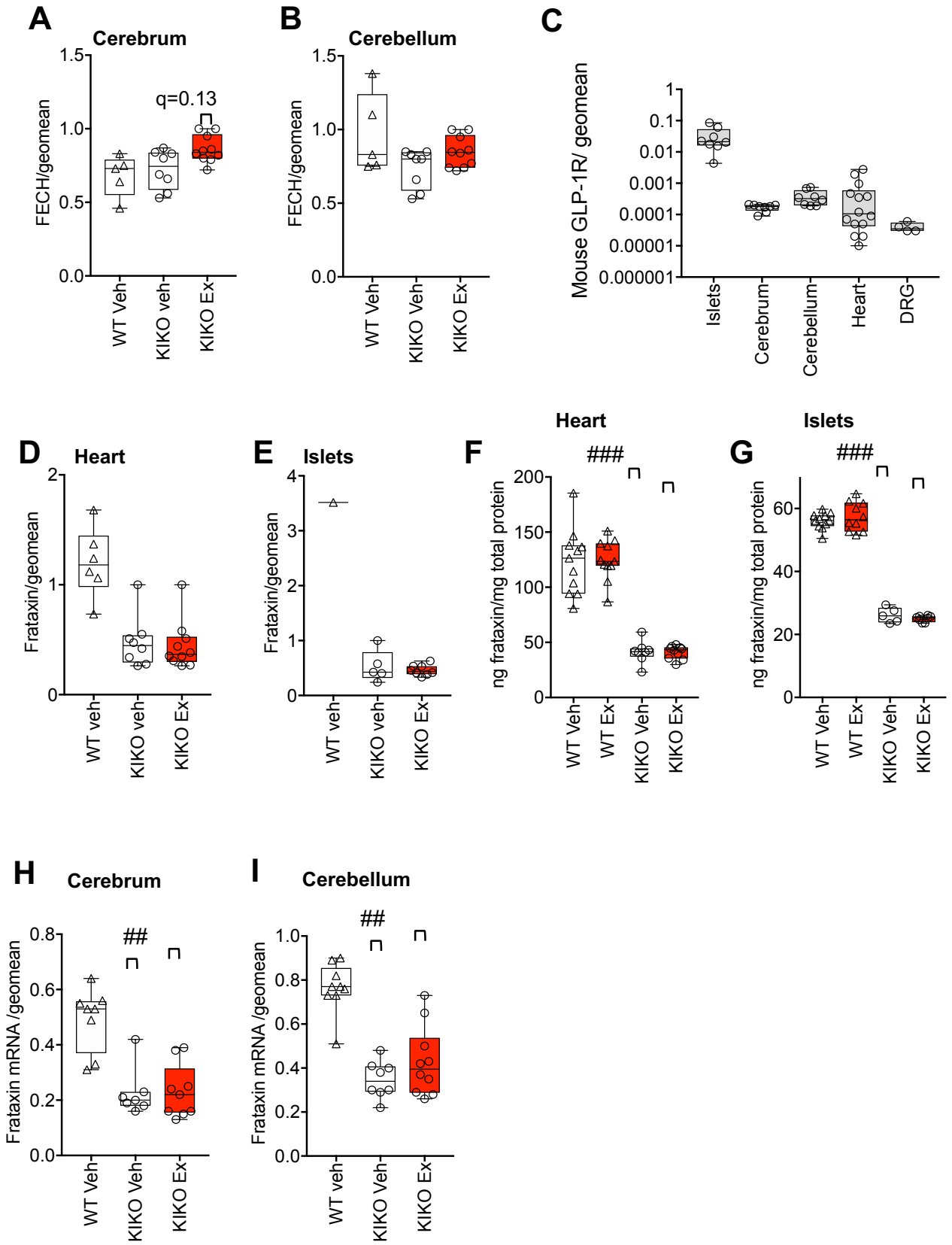


**Figure S3. mRNA and protein expression of frataxin and downstream targets in tissues from WT and KIKO mice treated or not with exenatide.** (A, B) Ferrochelatase (FECH) expression assessed by Western blot (n=5-10 per group). (C) GLP-1 receptor mRNA expression in different tissues measured by real-time PCR (n=4-14 per condition). DRG denotes dorsal root ganglia. (D-G) Frataxin protein expression in heart or islets measured by Western blot (D-E) or ELISA (F-G) (n=5-11 per group). Protein expression was normalized to the geometric mean of the reference proteins GAPDH and  $\alpha$ -tubulin (Western blot) or total protein (ELISA). (H-I) Frataxin mRNA expression measured by real-time PCR, normalized to the geometric mean of reference genes GAPDH and  $\beta$ -actin (n=7-10 per group). Data points represent samples from different mice. In the box plots the median is shown by a horizontal line; 25<sup>th</sup> and 75<sup>th</sup> percentiles are at the bottom and top of the boxes; whiskers represent minimum and maximum values. ##q<0.01, ###q<0.001 KIKO vs WT by Kruskal-Wallis test followed by Benjamini, Krieger and Yekutieli correction for multiple comparisons

Supplementary Figure 4

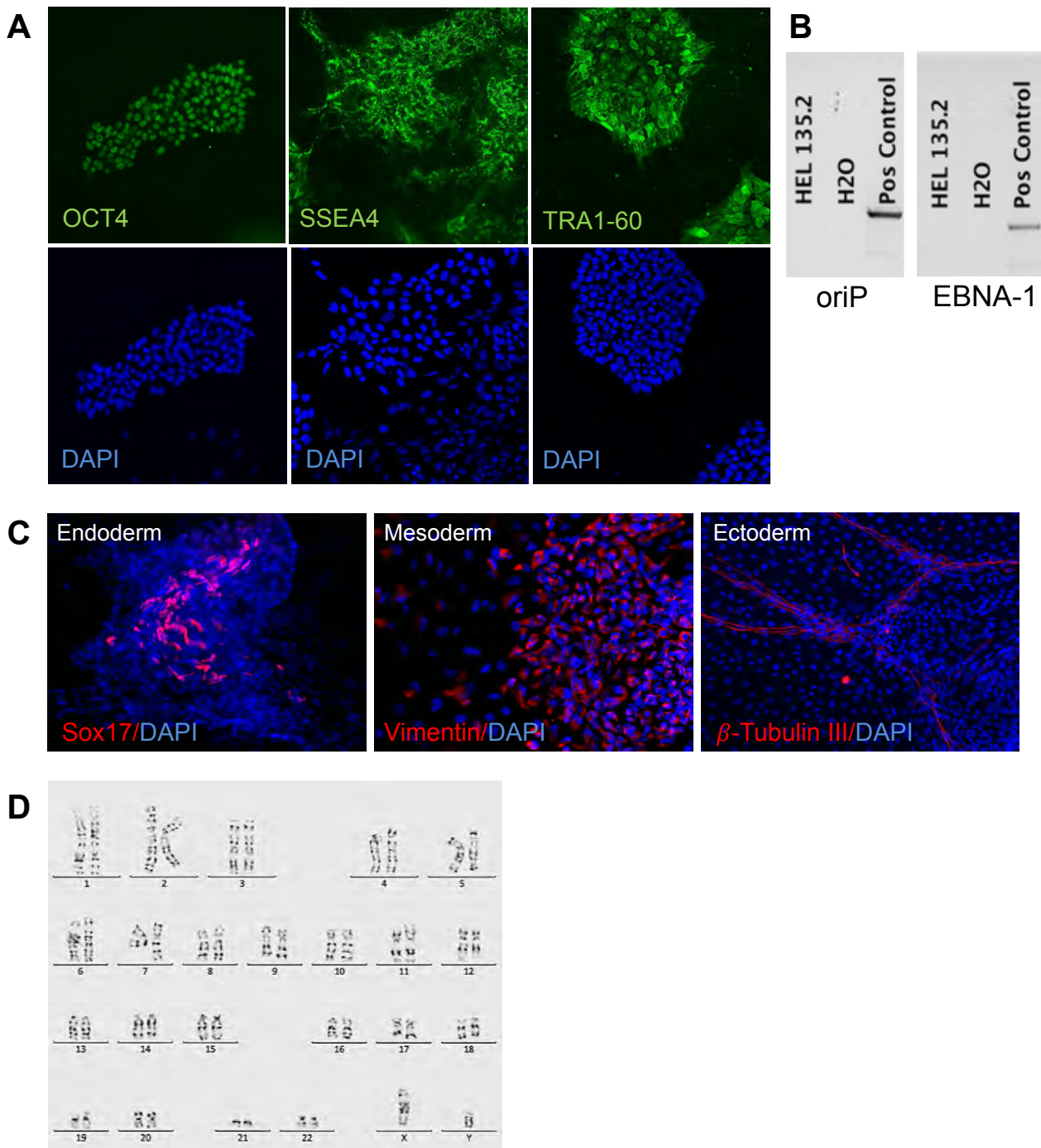


**Figure S4. Characterization of FRDA patient iPSC line HEL135.2.** (A) Immunofluorescent staining of iPSCs for the pluripotency markers OCT4, SSEA4 and TRA1-60. (B) PCR for the Epstein-Barr virus oriP/EBNA-1 viral elements, necessary for episomal vector maintenance and replication. The iPSC line Hel 135.2 showed absence of

oriP and EBNA-1 indicating that the vector had not integrated into the genome. cDNA from early passage Sendai vector-transduced fibroblasts were used as positive control (Pos Control). (C) Immunofluorescent analysis of embryoid bodies derived from iPSCs. SOX17, vimentin and  $\beta$ -tubulin III were used as markers of endoderm, mesoderm and ectoderm, respectively. Embryoid bodies were formed as previously described (1). Pictures were taken at 20x magnification. (D) iPSC karyotype showing no chromosomal alterations.

Supplementary Figure 5

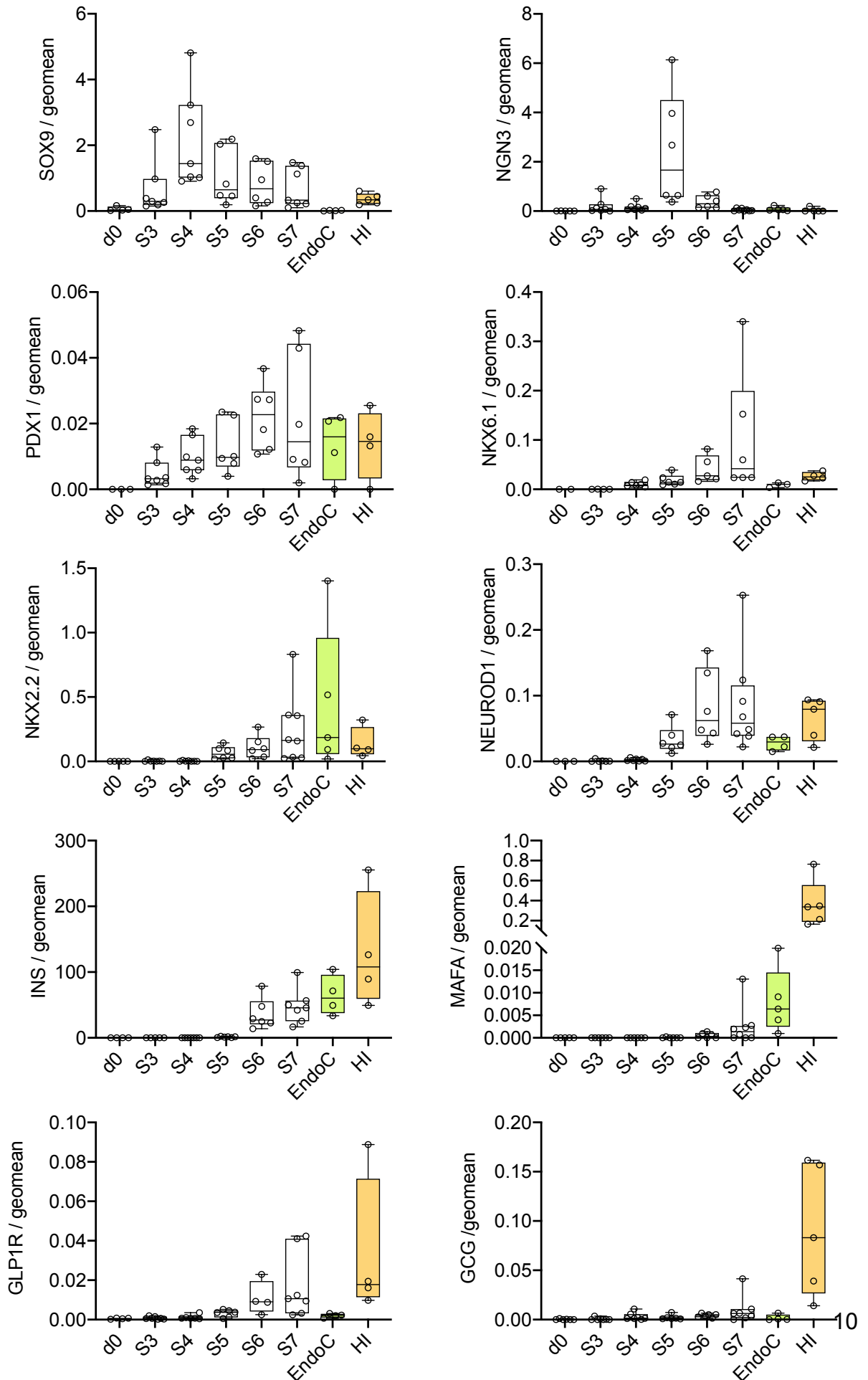


**Figure S5. Gene expression during iPSC differentiation into pancreatic  $\beta$ -cells.**

mRNA expression of FRDA patient cell line HEL135.2 at iPSC stage (d0) and across differentiation stages 3 through 7 (n=6-8). SOX9 and neurogenin3 (NGN3) are transiently expressed, followed by induction of downstream genes NeuroD1 and NKX2.2. PDX1, NKX6.1, INS, GCG and GLP1R mRNA expression are progressively induced. MAFA expression remains very low. mRNA expression in clonal human EndoC- $\beta$ H1  $\beta$ -cells (green bars) and adult organ donor human islets (HI, orange bars, n=4-5) is shown for comparison. Data were normalized to the geometric mean of reference genes GAPDH and  $\beta$ -actin. Individual data points represent independent samples. The median is shown by horizontal lines in the box plots; 25<sup>th</sup> and 75<sup>th</sup> percentiles are at the bottom and top of the boxes; whiskers represent minimum and maximum values.

## Supplementary Figure 6

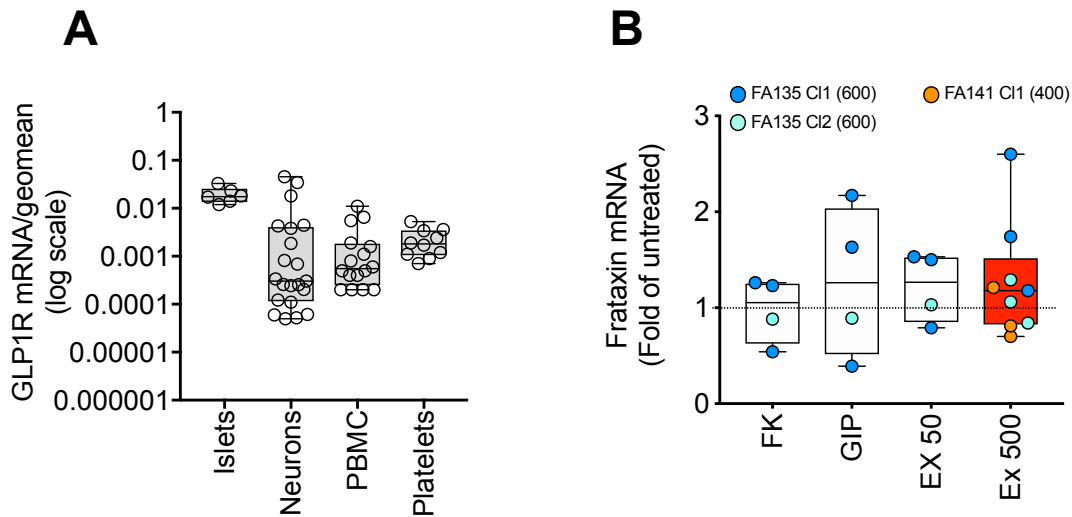


**Figure S6. Frataxin and GLP-1 receptor mRNA expression in human samples.** (A) GLP-1 receptor mRNA expression examined by real-time PCR and normalized to the geometric mean of the reference genes GAPDH, OAZ1 and  $\beta$ -actin (n=6-21). (B) Frataxin mRNA expression in iPSC-derived neurons from 2 FRDA patients (FA135 and FA141), treated or not for 72 hours with forskolin (20 mM, FK), [D-Ala<sup>2</sup>]GIP<sub>1-42</sub> (100 nM, GIP) or exenatide (50 nM, Ex 50, or 500 nM, Ex 500) (n=4-9 per group). Data were normalized to the reference gene  $\beta$ -actin and expressed as fold of untreated samples. Individual data points represent independent samples. Patients and clones are shown in different colors; the smaller GAA expansion size in *FXN* is shown in brackets. The median is shown by horizontal lines in the box plots; 25<sup>th</sup> and 75<sup>th</sup> percentiles are at the bottom and top of the boxes; whiskers represent minimum and maximum values.

# Supplementary Figure 7

A

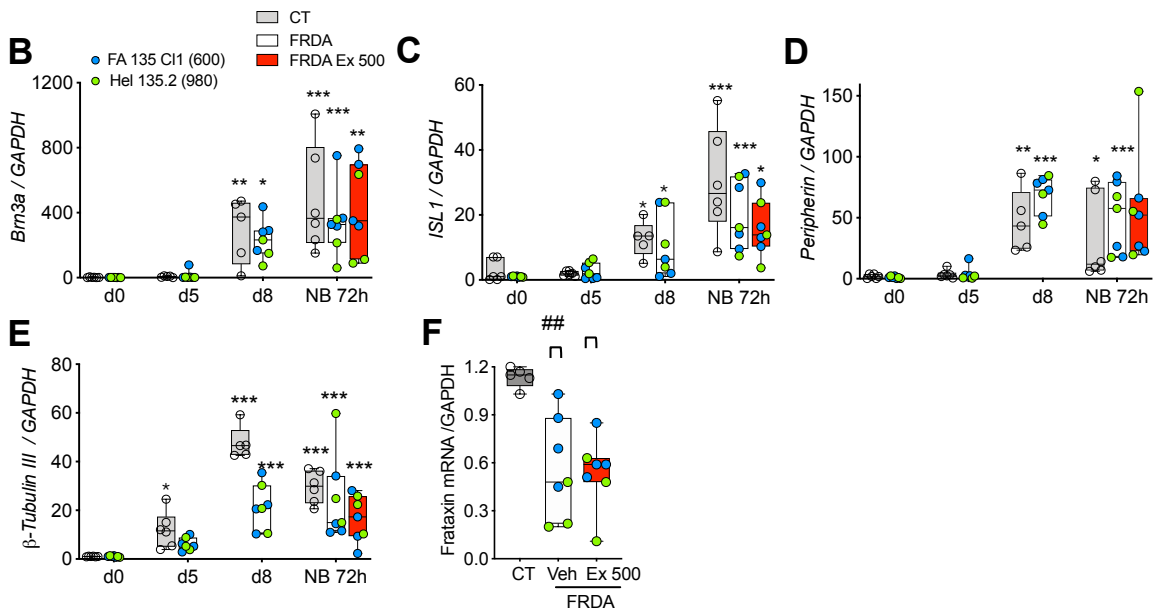
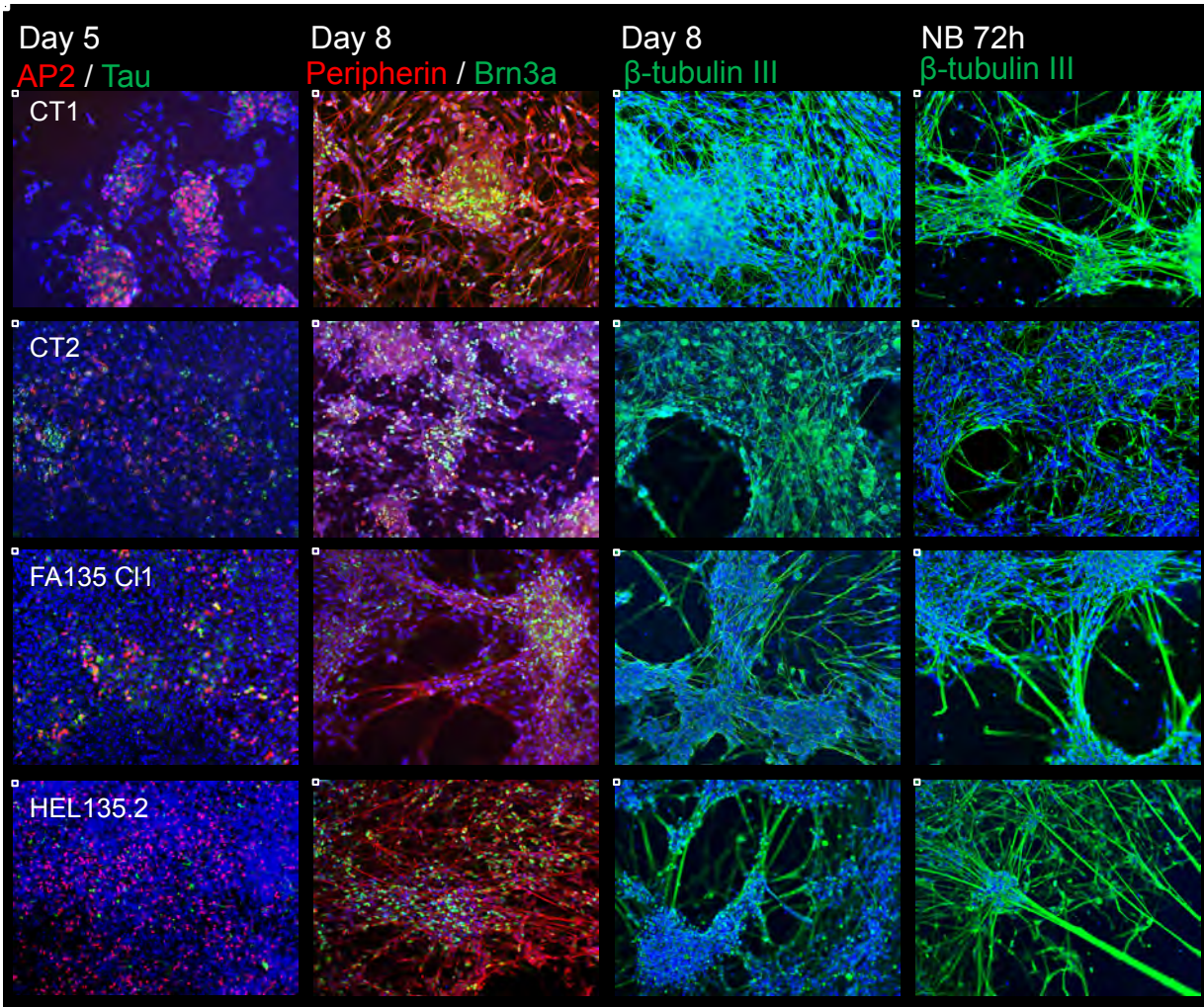


**Figure S7. iPSC differentiation into sensory neurons.** (A) Representative immunofluorescence images of control (CT1 and CT2) and FRDA patient cells (FA135 C11 and HEL135.2) during sensory neuron differentiation. Pictures were taken at 20x magnification. Expression of the sensory neuron markers Brn3a (*POU4F1*) and peripherin (*PRPH*) after 8 days of differentiation, and the neuron-specific cytoskeleton marker  $\beta$ -tubulin III at day 8 and after 72-hour culture in neurobasal medium (NB 72h). Images are representative of 7 similar experiments. (B-E) mRNA expression of the sensory neuron-specific transcription factors Brn3a and ISL1, and the cytoskeleton markers peripherin and  $\beta$ -tubulin III at day 5 and 8 of differentiation in control and FRDA patient cells exposed or not to exenatide 500 nM (Ex 500) (n=5-7 per group). (F) Frataxin mRNA expression in sensory neurons from 2 controls and 2 FRDA patients treated or not (Veh) with 500 nM exenatide for 72 hours in neurobasal medium (n=5-7 per group). mRNA expression was analyzed by real-time PCR and normalized to the reference gene GAPDH. Data is represented using box plots. The horizontal line in the box corresponds to the median, 25<sup>th</sup> and 75<sup>th</sup> percentiles are at the bottom and top of the box; whiskers indicate minimum and maximum values. Data points represent independent experiments. Patients are shown in different colors; the smaller GAA expansion size in *FXN* is shown in brackets. \*p<0.05, \*\*p<0.005, \*\*\*p<0.001 d8 or NB 72h vs d0 by mixed-effects analysis followed by Tukey correction for multiple comparisons, ##q<0.01 by Kruskal-Wallis test followed by Benjamini, Krieger and Yekutieli correction for multiple comparisons..

# Supplementary Figure 8

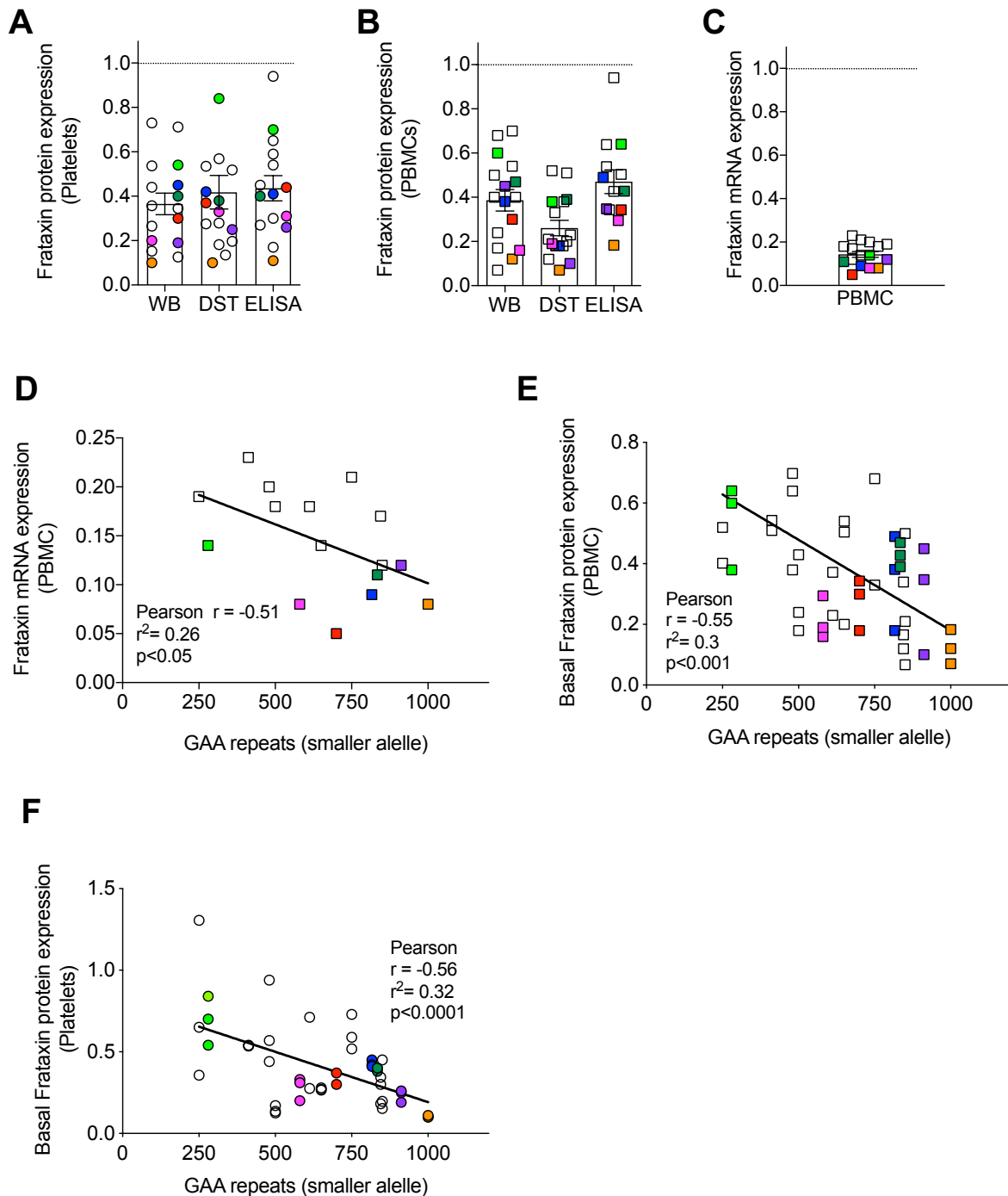


**Figure S8. Baseline frataxin protein and mRNA levels in platelets and PBMCs and correlation with GAA repeat size.** Frataxin protein (A, B, D) and mRNA expression (C, E) in platelets and PBMCs from FRDA patients at baseline (before exenatide treatment) (n=16). Frataxin protein expression was measured by Western blot, dipstick and ELISA

and normalized to the geometric mean of GAPDH,  $\beta$ -actin and COX IV in Western blots, and to total protein for dipstick and ELISA. Frataxin mRNA expression was assessed by real-time PCR and normalized to the geometric mean of GAPDH and  $\beta$ -actin. Frataxin mRNA and protein levels were normalized to average frataxin expression of 2 healthy control individuals, represented as 1 (dotted line). Correlation between baseline frataxin mRNA (D) or protein expression (E-F) and the smaller GAA repeat number in *FXN* in PBMCs (squares) and platelets (circles). The protein expression data include measurements with the 3 different methods. Patients from the exenatide and liraglutide arms are shown in colored and white symbols, respectively.

## Supplementary Figure 9

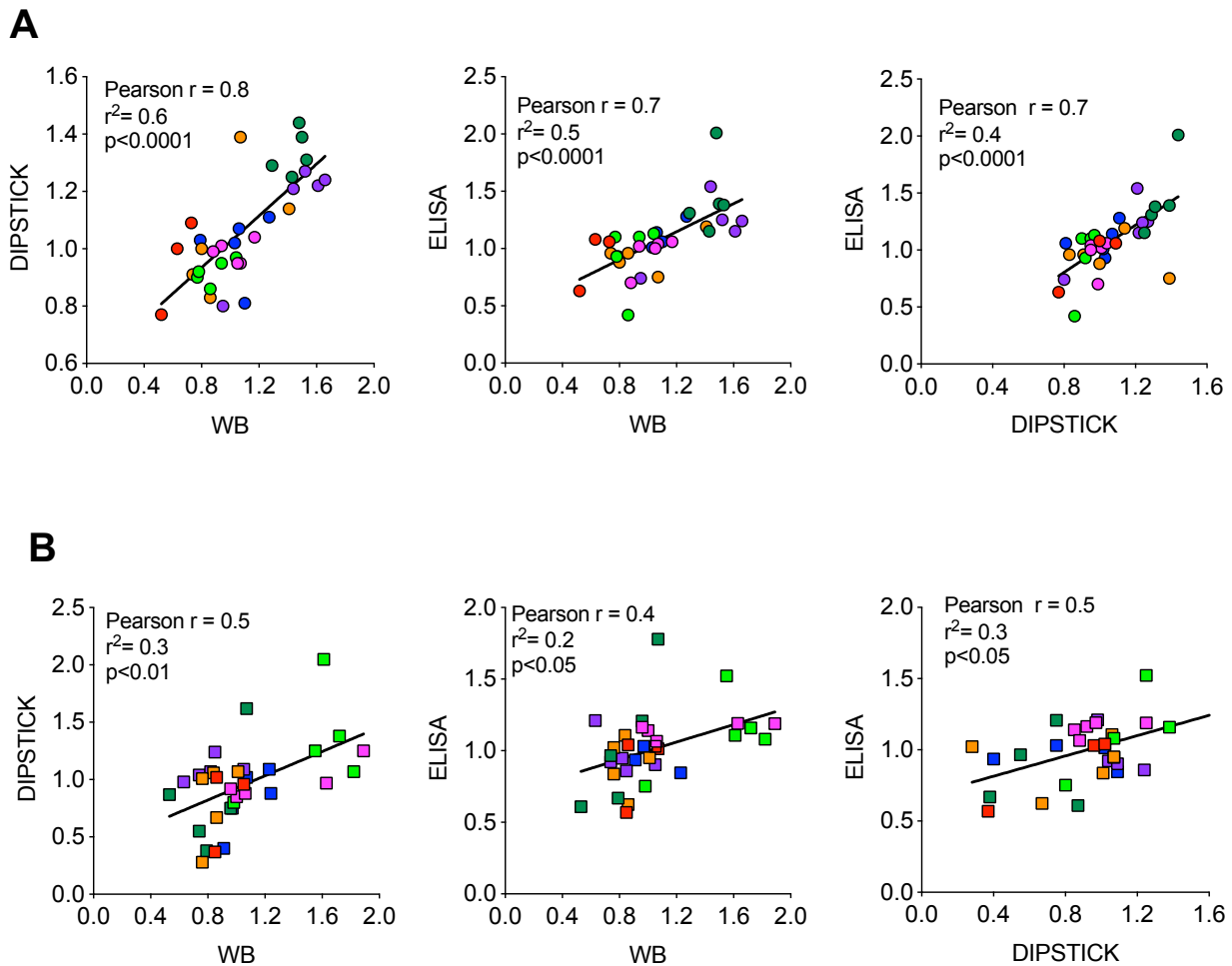


**Figure S9. Frataxin protein expression assessed by different methods.** Correlation between frataxin protein levels assessed by dipstick, Western blot (WB) and ELISA in platelet (A) and PBMC (B) samples over the 5 weeks of exenatide treatment (n=7 patients). Data is expressed as fold change compared to baseline frataxin levels. Different colors represent individual patients.

# Supplementary Figure 10

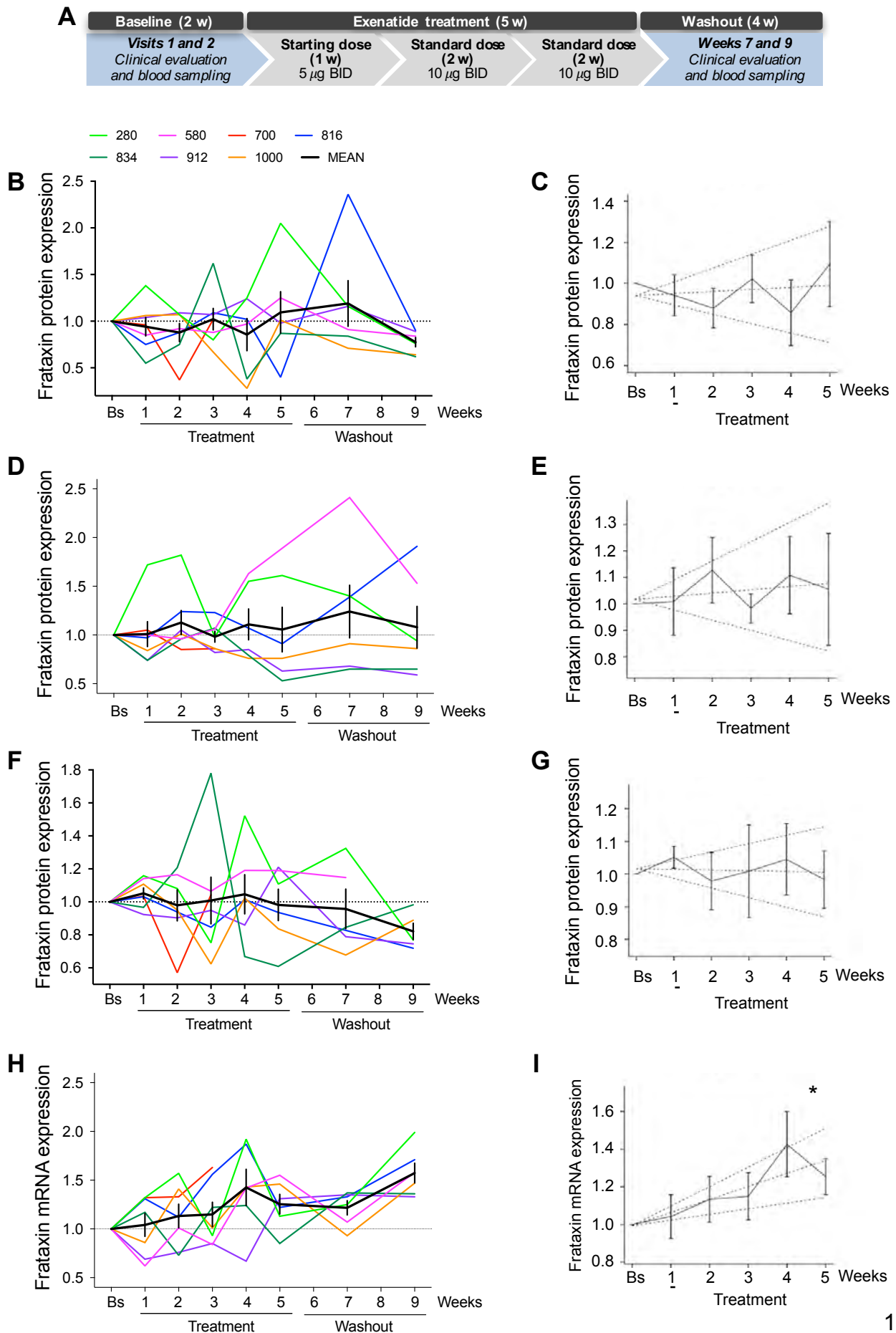


**Figure S10. Frataxin mRNA and protein expression in FRDA patients' PBMCs.** (A) Schematic representation of the pilot clinical trial. (B, D, F, H) Spaghetti plots of the changes in frataxin expression relative to baseline (Bs) in PBMCs over a 5-week treatment with exenatide followed by a 4-week washout. Frataxin protein was measured by dipstick (B, C), Western blot (D, E) and ELISA (F, G), and mRNA by real-time PCR (H, I). Frataxin mRNA expression was normalized to the geometric mean of GAPDH and  $\beta$ -actin. Colored lines represent individual patients (n=7), with the smaller GAA repeat length in *FXN* shown for each at the top of Panel B. The thick black lines indicate the mean $\pm$ SE for each time point. (C, E, G, I) Statistical analysis: the dashed lines indicate the non-parametric trend line fitted to the mean for each data point (solid black line) and the 95% confidence intervals generated by bootstrapping (n=1000). \*p<0.05 for a sustained increase in frataxin mRNA expression calculated by Fisher transformation.

**Table S1: Antibodies**

Peptide/protein target	Antibody name	Manufacturer, catalogue #	Species raised in; mono- or polyclonal	Dilution	RRID
Frataxin	Frataxin Antibody (H-155)	Santa Cruz Biotechnology, TX, USA, Cat# sc-25820	Rabbit, polyclonal	1:1000	AB_2110677
Aconitase	Anti-Aconitase 2 antibody	Abcam, UK, Cat# ab71440	Rabbit, polyclonal	1:500	AB_1267614
NDUFS3	NDUFS3 Polyclonal Antibody	Thermo Fisher Scientific, MA, USA, Cat# PA5-29747	Rabbit, polyclonal	1:1000	AB_2547221
Lipoic acid	Anti-Lipoic Acid Rabbit pAb antibody	Millipore, MA, USA, Cat# 437695-100UL	Rabbit, polyclonal	1:1000	AB_10683357
COX IV	COX IV Antibody	Cell signalling, Danvers, MA, UK, Cat# 4844	Rabbit, polyclonal	1:1000	AB_2085427
GAPDH	Anti-G3PDH Human Polyclonal Antibody	Trevigen, Gaithersburg, MD, USA, Cat# 2275-PC-020	Rabbit, polyclonal	1:1000	NA
$\alpha$ -Tubulin	Monoclonal Anti- $\alpha$ -Tubulin antibody	Sigma, Bornem, Belgium, Cat# T9026	Mouse, monoclonal	1:5000	AB_477593
Cleaved caspase 3	Cleaved Caspase-3 (Asp175)	Cell signalling, Danvers, MA, UK, Cat# 9661	Rabbit, polyclonal	1:100	AB_2341188
Insulin	FLEX Polyclonal Guinea Pig Anti-Insulin, Ready-to-Use	DAKO, Glostrup, Denmark, Cat# IR00261-2	Guinea pig, polyclonal	/	NA
OCT-3/4	Monoclonal Mouse Anti-OCT3/4 antibody	Santa Cruz Biotechnology, TX, USA, Cat# sc-5279	Mouse, Monoclonal	1:250	AB_628051
NKX6.1	Purified Mouse Anti-Nkx6.1	BD Biosciences, Belgium, Cat# 563022	Mouse, Monoclonal	1:250	NA
PDX1	Polyclonal Goat anti-PDX1- antibody	R&D System, UK, Cat# AF2419	Goat, Polyclonal	1:500	AB_355257
Glucagon	Monoclonal Anti-Glucagon-Antibody	Sigma, Bornem, Belgium, Cat# G2654	Mouse, Monoclonal	1:1000	AB_259852
SOX17	Polyclonal Goat IgG	R&D System, UK, Cat# AF1924	Goat, polyclonal	1:500	AB_355060
Anti-mouse IgG	Peroxidase AffiniPure F(ab') <sub>2</sub> Fragment Donkey Anti-Mouse IgG (H+L)	Jackson ImmunoResearch Laboratories, Wes Grove, PA, USA, Cat# 715-036-150	Polyclonal	1:5000	AB_2340773
Vimentin	Anti-vimentin antibody	Abcam, ab137321	Polyclonal	1:100	NA
Beta tubulin III	Anti-beta-Tubulin III antibody	Sigma, Bornem, Belgium, T8660	Monoclonal	1:100	AB_477590
TRA1-60	TRA-1-60 Monoclonal Antibody, IgM	ThermoFisher Scientific, MA, USA, Cat# MA1-023X	Monoclonal	1:125	AB_2536705
Anti-Human SSEA-4	Anti-Human SSEA-4 Antibody, IgG	ThermoFisher Scientific, MA, USA, Cat# MC-813-70	Mouse, monoclonal	1:500	AB_528477
Anti-rabbit IgG	Peroxidase AffiniPure F(ab') <sub>2</sub> Fragment	Jackson ImmunoResearch	Polyclonal	1:5000	AB_2340590

	Donkey Anti-Rabbit IgG (H+L)	Laboratories, Wes Grove, PA, USA, Cat# 711-036-152			
Goat anti-guinea pig IgG	Goat anti-Guinea Pig IgG (H+L) Highly Cross-Adsorbed Secondary Antibody, Alexa Fluor 488	Life technologies, USA, Cat# A11073	Goat, polyclonal	1:500	AB_2534117
Goat anti-rabbit IgG	Goat Anti Rabbit IgG H&L (Alexa Fluor 488)	Thermo Fisher, MA, USA, Cat# R37116	Goat, polyclonal	1:500	AB_2556544
Goat anti-rabbit IgG	Goat anti-Rabbit IgG (H+L) Highly Cross-Adsorbed Secondary Antibody, Alexa Fluor 568	Life technologies, USA, Cat# A11036	Goat, polyclonal	1:500	AB_2534094
Donkey Anti-Mouse IgG	Donkey anti-Mouse IgG (H+L) Highly Cross-Adsorbed Secondary Antibody, Alexa Fluor 488	Life technologies, USA, Cat# A21202	Donkey	1:500	AB_141607
Donkey Anti-Goat IgG	Donkey anti-Goat IgG (H+L) Cross-Adsorbed Secondary Antibody, Alexa Fluor 546	Life technologies, USA, Cat#:A11056	Donkey	1:500	AB_2534103
Donkey Anti-Guinea Pig IgG	Alexa Fluor488-conjugated AffiniPure Donkey Anti-Guinea Pig (H+L) antibody	Jackson ImmunoResearch Laboratories, Wes Grove, PA, USA, Cat# 706-545-148	Donkey	1:500	AB_2340472
Rabbit Anti-Mouse IgG	Donkey anti-Goat IgG (H+L) Cross-Adsorbed Secondary Antibody, Alexa Fluor 568	Life technologies, USA, Cat# A11061	Rabbit	1:500	AB_2534108

NA= not available

**Table S2:** Sequence of mouse and human primers used for real-time PCR

Species	Gene	Forward sequence (5'→3')	Reverse sequence (5'→3')
Mouse	<i>Fxn</i>	ACGAGACAGCGTATGAAAGA	ACGCCATCCCAAAGAGAC
Mouse	<i>Glp1r</i>	TGGGCAATCGGATGATGAG	ATCTCTATGAGGACGAGGG
Mouse	<i>Gapdh</i>	AACTTTGGCATTGTGGAAGG	GGATGCAGGGATGATGTTCT
Human	<i>FXN</i>	AAGCAGAGTGTCTATTTGATG	AAGAGTCCAGCGTTTCCTC
Human	<i>GLP1R</i>	AAGGACAACTCCAGCCTGC	ATGATGTAGAGGAACAGGAG
Human	<i>β-tubulin III</i>	AGATGTTTCGATGCCAAGAA	GGATCCACTCCACGAAGTA
Human	<i>ISL1</i>	GTAGAGATGACGGGCCTCAG	TTTCCAAGGTGGCTGGTAAC

*BRN3A*

Human	<i>(POU4F1)</i>	ACTCAGCCAGAGCACCATCT	TTTGAGGTCCAGTTTCTCGG
Human	<i>PRPH</i>	AAGACGACTGTGCCTGAGGT	TGCTCCTTCTGGGACTCTGT
Human	<i>GAPDH</i>	CAGCCTCAAGATCATCAGCA	TGTGGTCATGAGTCCTTCCA
Human	<i>ACTB</i>	CTGTACGCCAACACAGTGCT	GCTCAGGAGGAGCAATGATC
Human	<i>OAZ1</i>	GGATCCTCAATAGCCACTGC	TACAGCAGTGGAGGGAGACC
Human	<i>MAFA</i>	GCCAGGTGGAGCAGCTGAA	CTTCTCGTATTTCTCCTTGAC
Human	<i>PDX1</i>	AAAGCTCACGCGTGGAAA	GCCGTGAGATGTACTTGTTGA
Human	<i>NKX6.1</i>	GGGCTCGTTTGGCCTATT	CGTGCTTCTCCTCCACTT
Human	<i>NKX2.2</i>	GAACCCCTTCTACGACAGCA	ACCGTGCAGGGAGTACTGAA
Human	<i>NEUROD1</i>	CTATCACTGCTCAGGACCTACT	CCACTCTCGCTGTACGATTT
Human	<i>INS</i>	CCAGCCGCAGCCTTTGTGA	CCAGCTCCACCTGCCCA
Human	<i>GGC</i>	GCTAAACAGAGCTGGAGAGTAT	AAGCCCTCTTTGGGAACTT
Human	<i>NGN3</i>	GACGACGCGAAGCTCACCAA	TACAAGCTGTGGTCCGCTAT
Human	<i>SOX9</i>	ATCAAGACGGAGCAGCTGAG	GGCTGTAGTGTGGGAGGTTG

**Table S3:** Primers used in conventional PCR to generate standards

<b>Species</b>	<b>Gene</b>	<b>Forward sequence (5'→3')</b>	<b>Reverse sequence (5'→3')</b>
Mouse	<i>Fxn</i>	CCATTTGAACCTCCACTACC	TGTTTGGGGTCTGCTTGTTT
Mouse	<i>Glp1r</i>	TACTACTGGTTGCTGGTGG	ATGACAGGATGAAGATAAGT

Mouse	<i>Gapdh</i>	TAACATCAAATGGGGTGAGG	TGTTGCTGTAGCCGTATTCA
Human	<i>FXN</i>	AGCAGCATGTGGACTCTC	AAGGAGACATCATAGTCCTC
Human	<i>GLP1R</i>	AGAAATGGCGAGAATACCGAC	TGTGCTATACATCCACTTCAG
Human	<i>GAPDH</i>	CTGAGAACGGGAAGCTTGTC	AGGTCAGGTCCACCACTGAC
Human	<i>ACTB</i>	AAATCTGGCACCACACCTTC	CCGATCCACACGGAGTACTT
Human	<i>OAZ1</i>	CGGAGGTTTTCTGGTTTC	GGAGAACTGCAAAGCTGTCC
Human	<i>MAFA</i>	TCATCCGGCTCAAGCAGAAG	CGCCTAXAGGAAGAAGTCGG
Human	<i>PDX1</i>	CTGCCTTTCCCATGGATGAA	CTTGATGTGTCTCTCGGTCAAG
Human	<i>NKX6.1</i>	AAACACACGAGACCCACTTT	GCTTATTGTAGTCGTTCGTCTC
Human	<i>NKX2.2</i>	AAGACGGGGTTTTCCGGTCAA	TGTCATTGTCCGGTGACTCG
Human	<i>NEUROD1</i>	CTATCACTGCTCAGGACCTACT	GTCATCCTCTCTTCTCTTCT
Human	<i>INS</i>	TGTCCTTCTGCCATGGC	CCATCTCTCTCGGTGCA
Human	<i>GCG</i>	GGGAGAGGGAAGTCATTTGTAA	GTAGAACAGAGGAGGTGAAGAG
Human	<i>NGN3</i>	AAGAGCGAGTTGGCACTGAG	GGAGACTGGGGAGTAGAGGG
Human	<i>SOX9</i>	TGGATGTCCAAGCAGG	GAGCTGGAGTTCTGGTGGTC
	OriP	TTCCACGAGGGTAGTGAACC	TCGGGGGTGTTAGAGACAAC
	EBNA-1	ATCGTCAAAGCTGCACACAG	CCCAGGAGTCCCAGTAGTCA

---

## References

1. Cosentino C, Toivonen S, Diaz Villamil E, Atta M, Ravanat JL, Demine S, Schiavo AA, Pachera N, Deglasse JP, Jonas JC, et al. Pancreatic  $\beta$ -cell tRNA

hypomethylation and fragmentation link TRMT10A deficiency with diabetes. *Nucleic Acids Res.* 2018;46(19):10302-18.